

ChemElectroChem

Supporting Information

Binder-Free N-Functionalized Carbon Electrodes for Oxygen Evolution Reaction

Feihong Song⁺, Jan W. Straten⁺, Yang-Ming Lin, Yuxiao Ding, Robert Schlögl, Saskia Heumann,^{*} and Anna K. Mechler^{*}

Table S1. HTC and NHTC electrodes synthesis process. HT stands for hydrothermal treatment.

Sample name	Description of synthesis process	Annealing temp.
HTC-250	92.5 g glucose in 360 mL water HT at 250 °C for 6 h	1000 °C
NHTC-low-180	92.5 g glucose and 12 g urotropine in 360 mL water HT at 180 °C for 6 h	1000 °C
NHTC-low-250	92.5 g glucose and 12 g urotropine in 360 mL water HT at 250 °C for 6 h	1000 °C
NHTC-high-180	12 g glucose and 37.3 g urotropine in 360 mL water HT at 180 °C for 6 h	1000 °C

All chemicals were of analytical grade. D-(+)-Glucose ($\geq 99,5\%$, GC) was purchased from Sigma-Aldrich. Hexamethylenetetramine ($\geq 99\%$, urotropine) was supplied from Carl Roth Chemicals GmbH (Karlsruhe, Germany). The starting materials were dissolved in distilled water and stirred to form a homogeneous solution. The solution was then transferred to Teflon lined stainless steel autoclaves (50 mL volume) and heated to 180 or 250 °C for 6h (ramping rate 5 °C/s). The HTC materials were recovered by filtration and washing by DI water for several times. The HTCs were pelletized with a pressure of 10 t within 2-3 min and thermally annealed at 1000 °C for 5 h in inert atmosphere with an argon flow of 520 mL·min⁻¹.

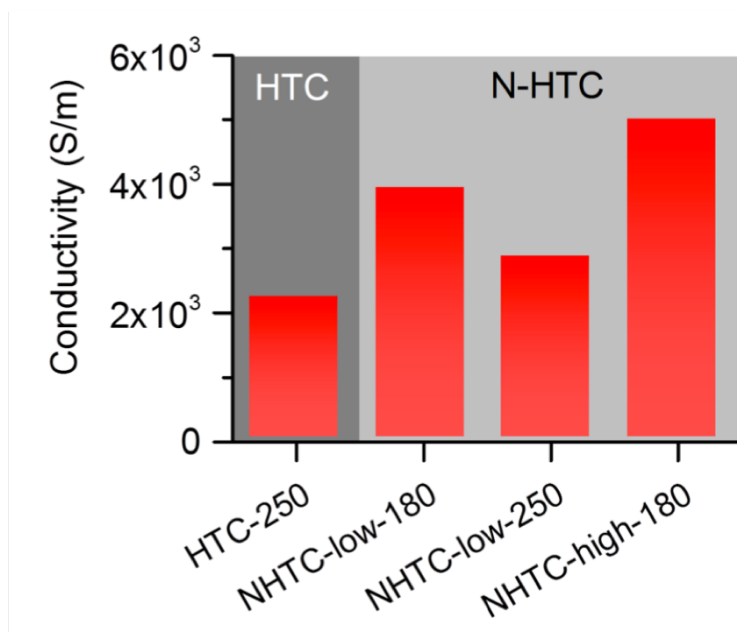


Figure S1. Van der Pauw conductivity measurements on different HTC and NHTC samples.

Conductivity measurements are carried out according to the van der Pauw measurement procedure. Four Ag conductive contacts were carefully painted on the edge of the HTC/NHTC pellet separated by 90°. By introducing N into the system, higher conductivity can be achieved. Among the NHTC samples, the one with higher N content (NHTC-high-180) has the highest conductivity, which might be caused by the synergistic effect of n-type doping of N and higher sp² carbon content (Figure S1).^[1]

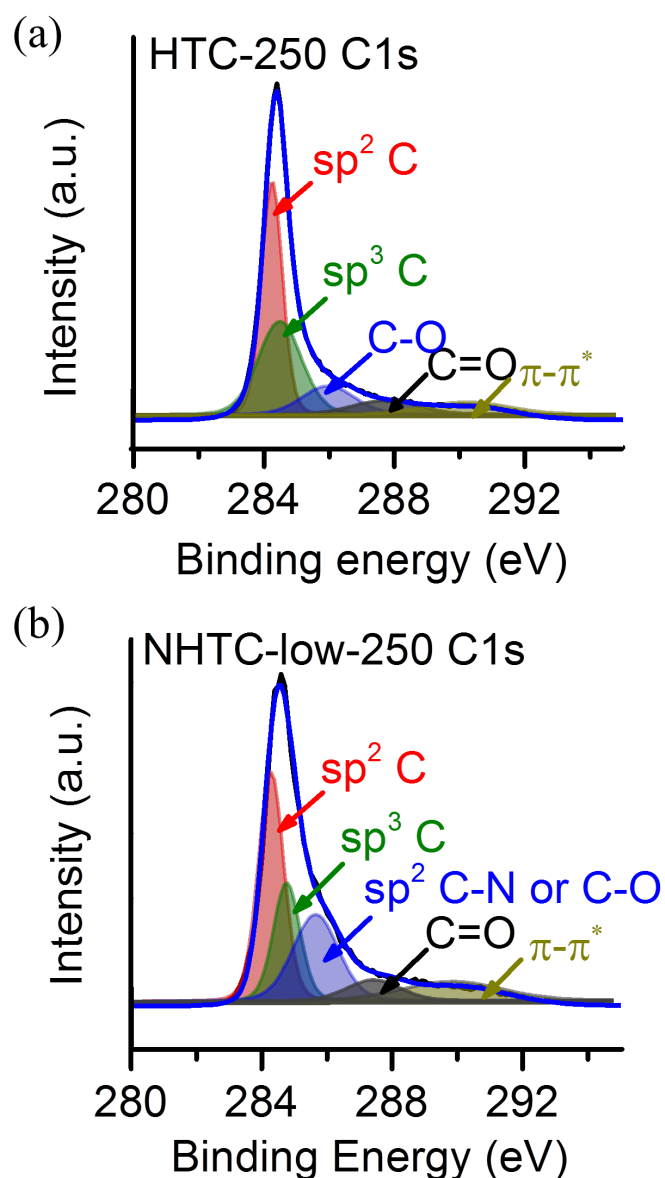


Figure S2. XPS C1s core level X-ray photoelectron spectra for a) HTC-250 and b) NHTC- low-250.

For both HTC-250 and NHTC-low-250, the primary C1s peak appears at 284.3 eV, which can be assigned to sp^2 C. (a) HTC-250 spectra is splitted into 5 regions, including sp^2 hybridized C (284.3 eV), sp^3 hybridized C (284.6 eV), C-O (286.1 eV), C=O (287.9 eV) and $\pi-\pi^*$ satellite (290.4eV). Only limited amount of oxygen-bonded carbon exist in the HTC sample, which is in-line with the elemental analysis result. (b) The introduction of extra N species into the carbon structure makes the peak fitting problematic for NHTC-low-250. Nevertheless, the spectra is empirically separated into 5 regions: sp^2 hybridized C (284.3 eV), sp^3 hybridized C (284.6 eV), sp^2 C bonded with N atom or C-O (286.1 eV), C=O (287.6 eV) and $\pi-\pi^*$ satellite (290eV).

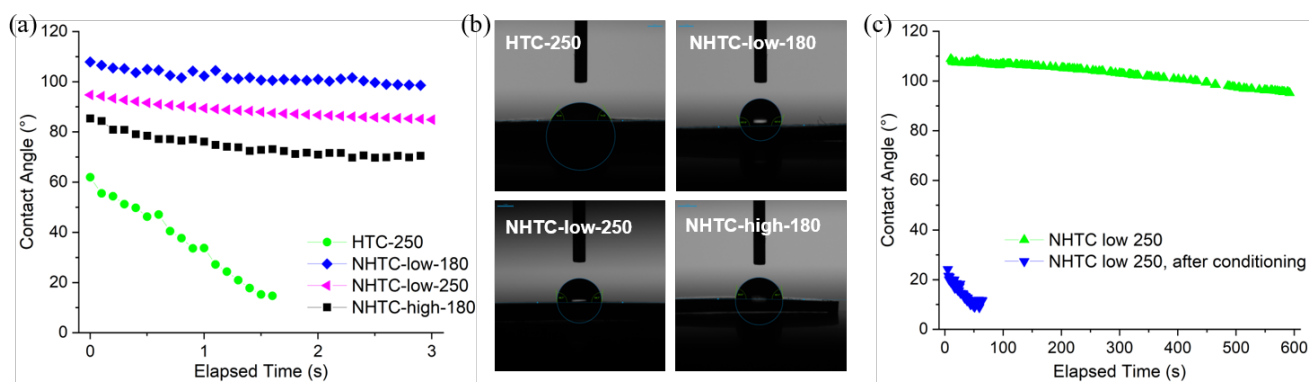


Figure S3. Contact angle measurement of different HTC and NHTC disc electrodes. a) Dynamic measurements for 3 s or until the droplet was fully absorbed; b) the first image captured for each of the different carbon disc electrodes; c) a long-term measurement over 10 min for NHTC-low-250 before the experiment as well as after the first conditioning step.

2 μL of deionized water is used for each measurement in a) and b). The images were captured with a frequency of 50 Hz for a total duration of 3 s. The pictures in b) are recorded immediately after the landing of the water droplet. For the longer experiment in c) 0.1 M KOH and a 10 μL droplet was used. The contact angle is determined using the elliptic fitting algorithm provided by KRÜSS GmbH.

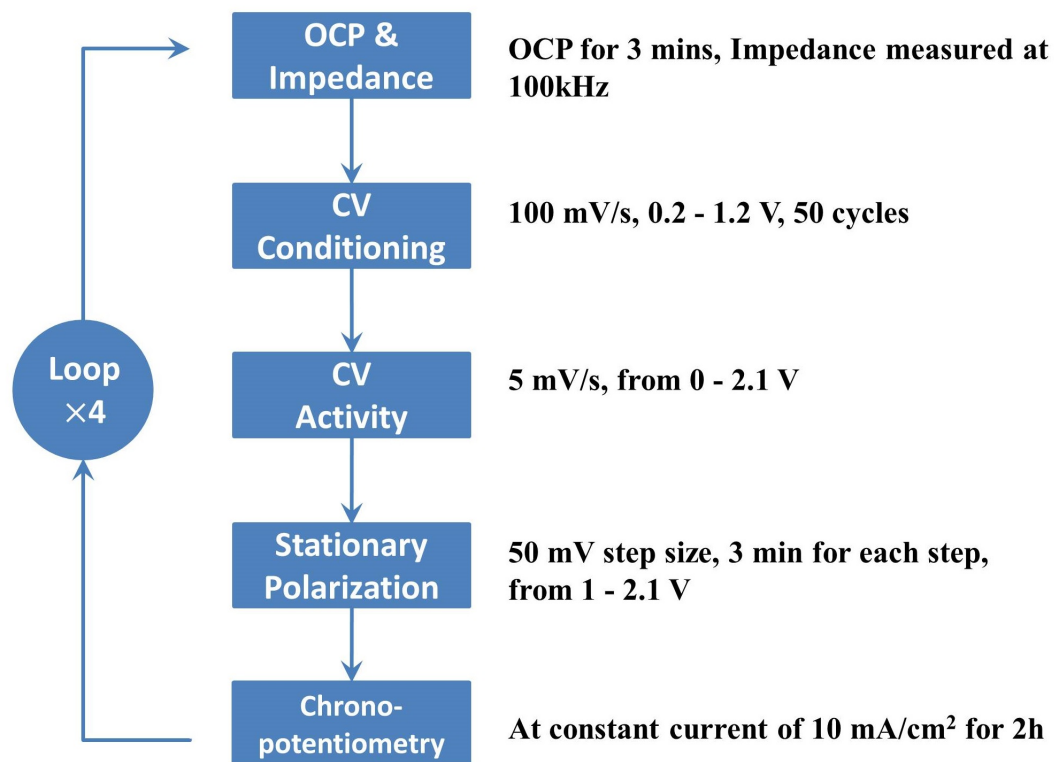


Figure S4. Electrochemical performance measurement protocol.

The KOH electrolyte concentration was 0.1 M. It was used as delivered and not further purified. The electrochemical measurement protocol contains four loops, each loop includes, in sequence: Impedance for IR compensation, capacitance/conditioning cyclic voltammetry (CV), activity CV, stationary polarization and chronopotentiometry (CP) tests. CP is a measure to evaluate the stability, by applying 10 mA/cm² for 2 h. To further monitor the properties change during the measurement, all sequences were repeated in total four times, which accumulated to a total measurement time of 18 h.

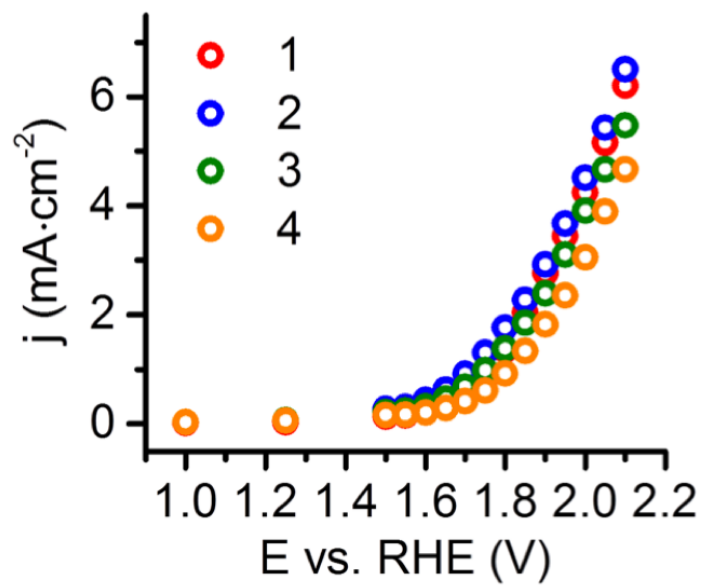


Figure S5. Stationary polarization measurement within four loops measurement protocol for NHTC-low-250 sample in Ar-purged electrolyte. The electrolyte was purged with Ar before (for 30 min) and during the measurement.

electrospray-ionization (Sol.: H2O + CH3OH) neg. ions
 characteristical ions
 61 = [(CO3)2- + (H)+] possible
 additional characteristical ions
 59, 75

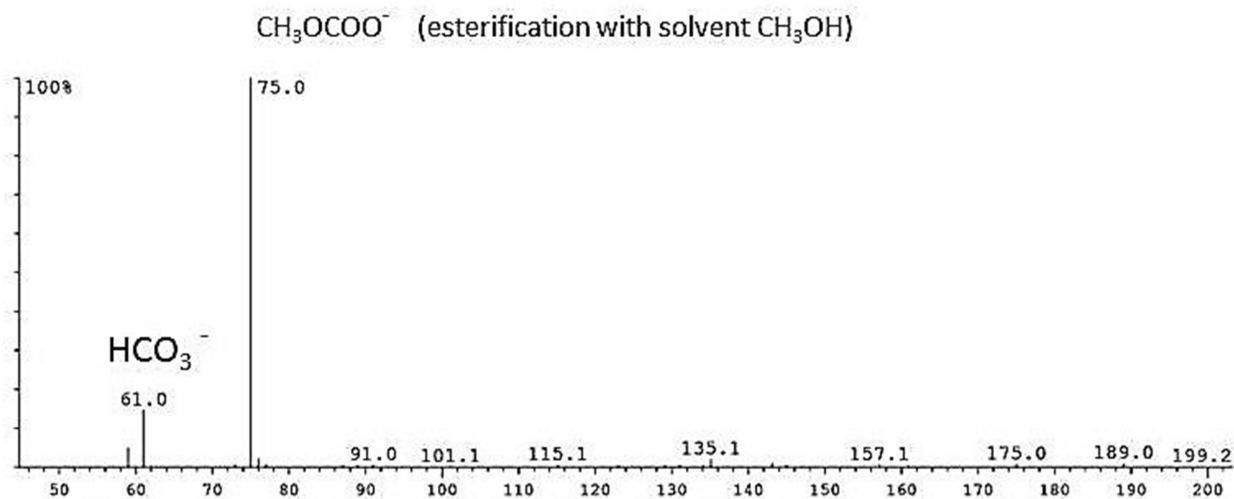


Figure S6. Electron spray ionization mass spectrometry (ESI-MS) for the electrolyte after operation of NHTC-low-250 sample. Methanol was used as the solvent to dilute the electrolyte.

ESI-MS was used to analyze the components in the electrolyte after full four loop measurement described in Figure S4. Two main peaks appears at $m/z = 61$ and $m/z = 75$, corresponding to HCO_3^{2-} and CH_3COO^- , respectively. HCO_3^{2-} is the direct product of CO_3^{2-} after the ionization process and CH_3COO^- is the indirect product of CO_3^{2-} reacting with the solvent methanol (CH_3OH) through esterification process (side reaction of the ionization process). Therefore, all the main peaks relate to CO_3^{2-} , which proves that the main component in the electrolyte is the carbonate ion. Small amount of soluble carbon molecules with greater m/z were also found. These molecules are most likely detached from the carbon backbone during the oxidation of carbon in alkaline media, which is also part of the carbon deactivation process, but in rather small contribution.

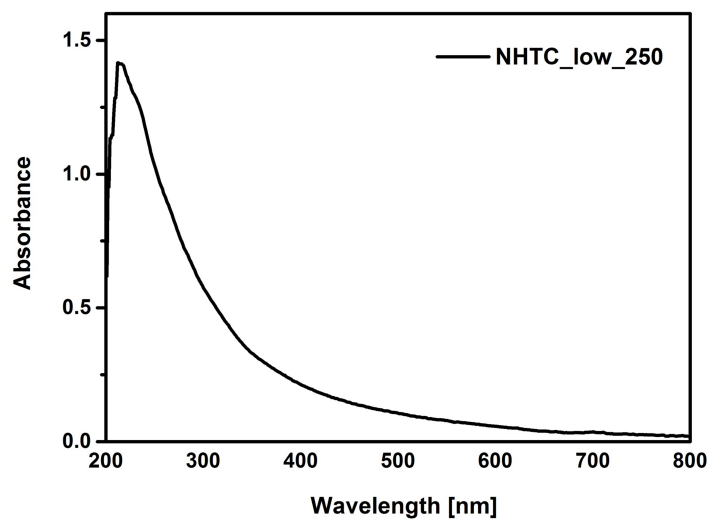


Figure S7. UV-Vis Spectroscopy of the electrolyte after electrochemical performance measurements.

The UV-Vis spectra clearly show broad peaks at around 220 nm for all the samples. The broad peak can be assigned to π - π^* transition of aromatic carbon molecules (e.g. humic acid) with various amount of benzene rings.

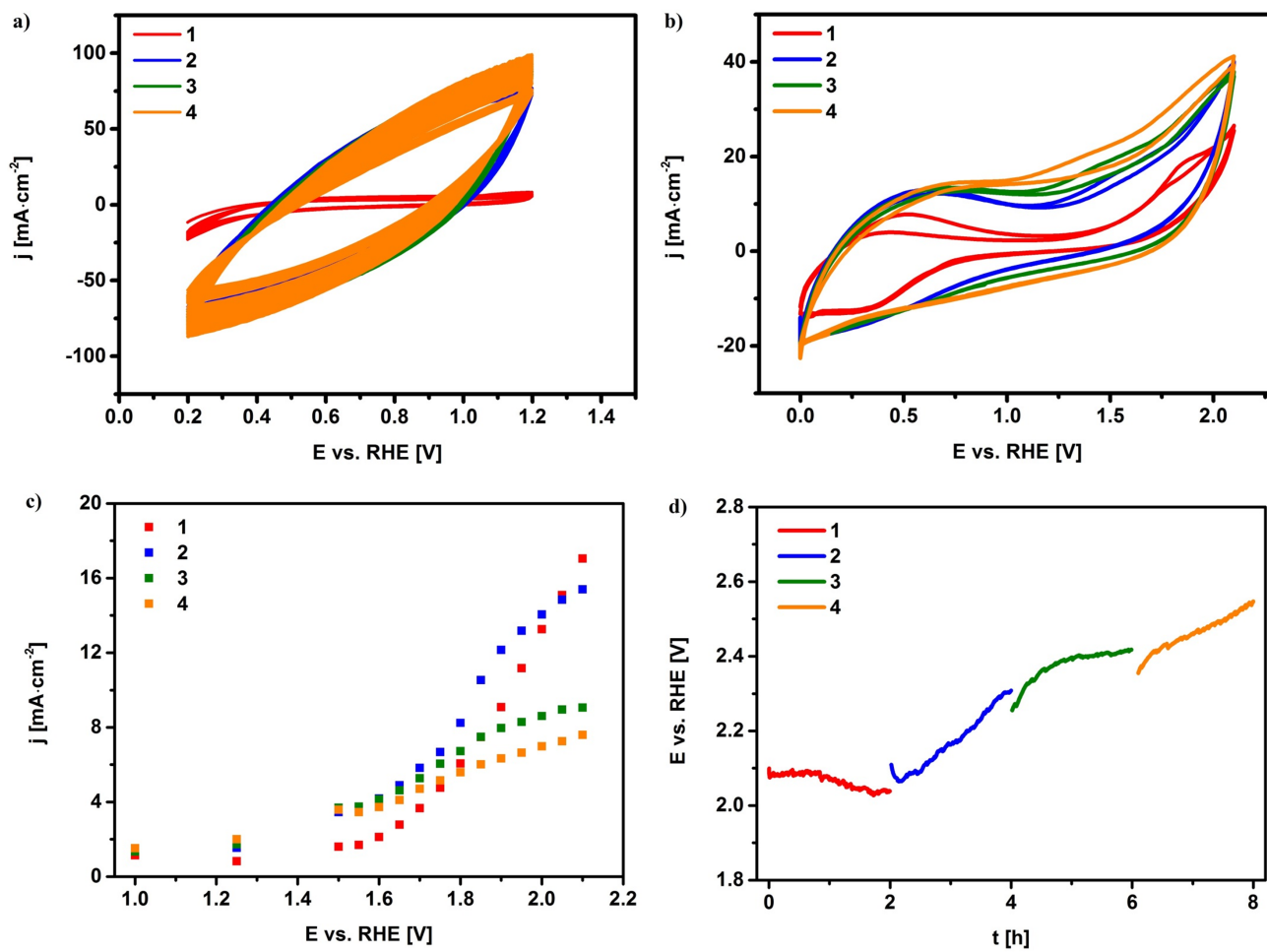


Figure S8. Electrochemical measurement results of HTC-250 (a) capacitance test, (b) activity test, (c) stationary polarization test, (d) chronopotentiometry test.

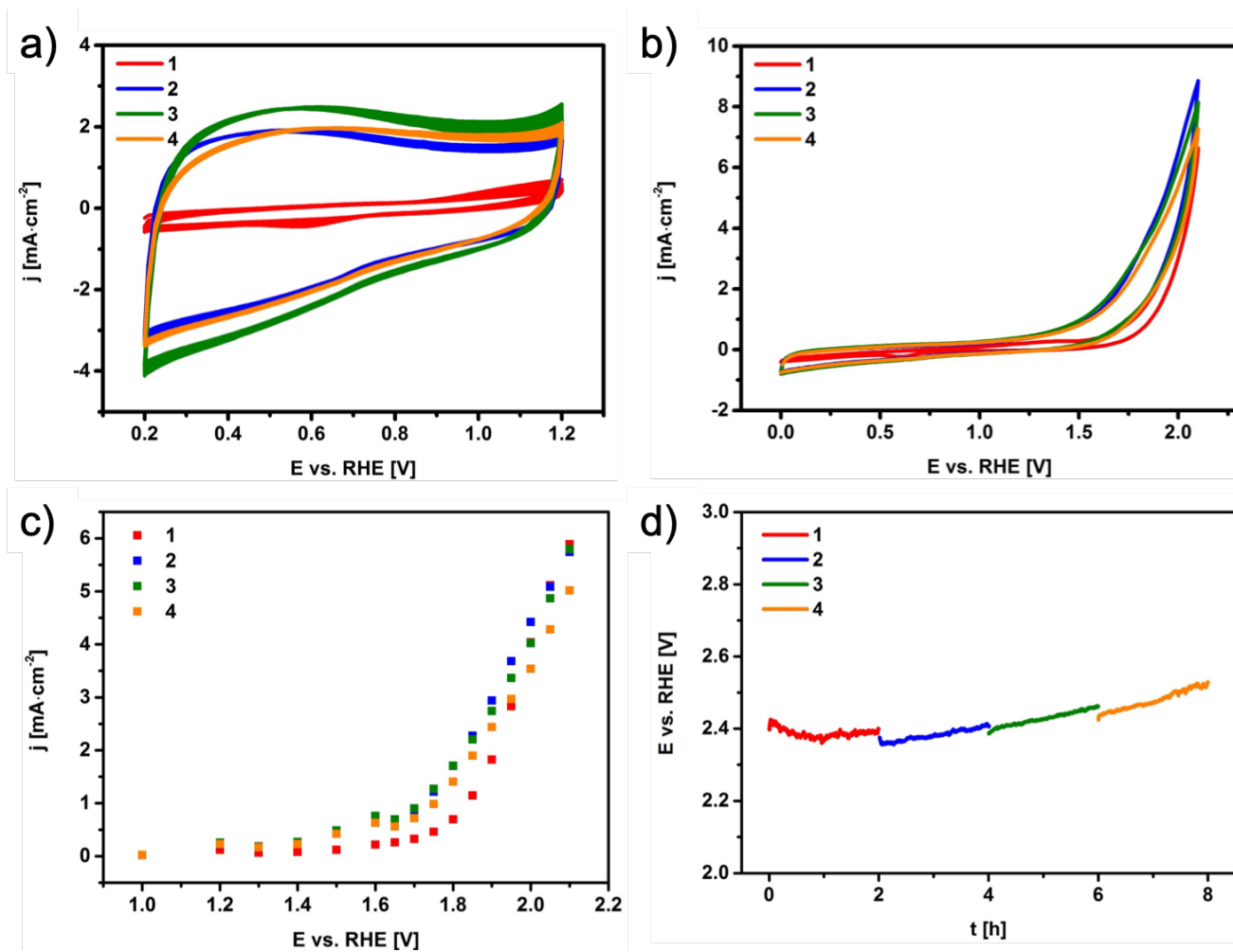


Figure S9. Electrochemical measurement results of NHTC-low-180 (a) capacitance test, (b) activity test, (c) stationary polarization test, (d) chronopotentiometry test.

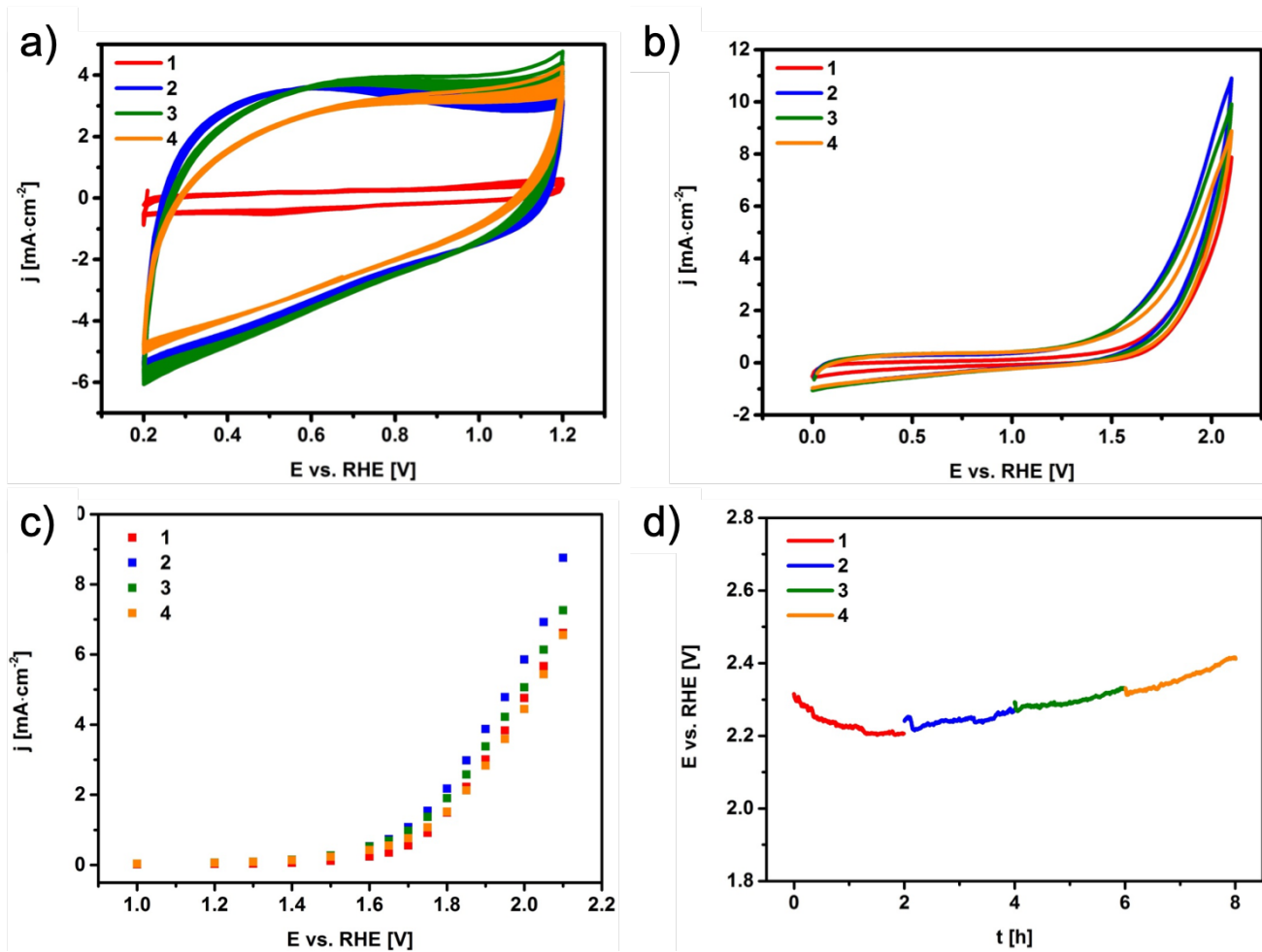


Figure S10. Electrochemical measurement results of NHTC-high-180 (a) capacitance test, (b) activity test, (c) stationary polarization test, (d) chronopotentiometry test.

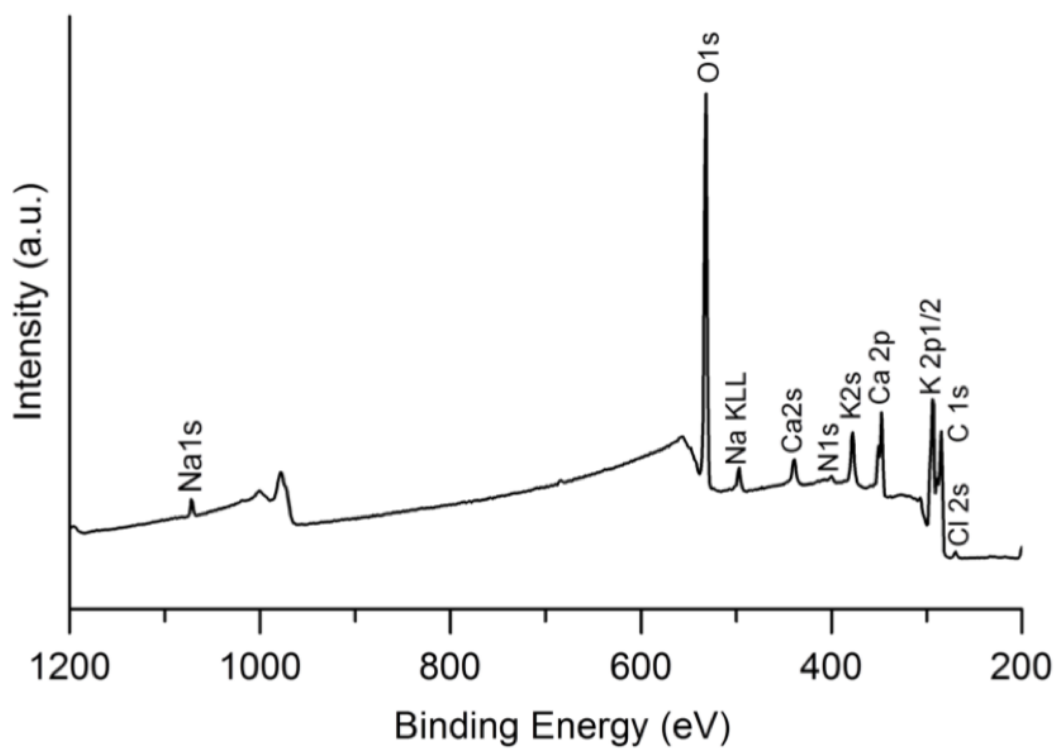


Figure S11. XPS survey of NHTC after four loops measurement.

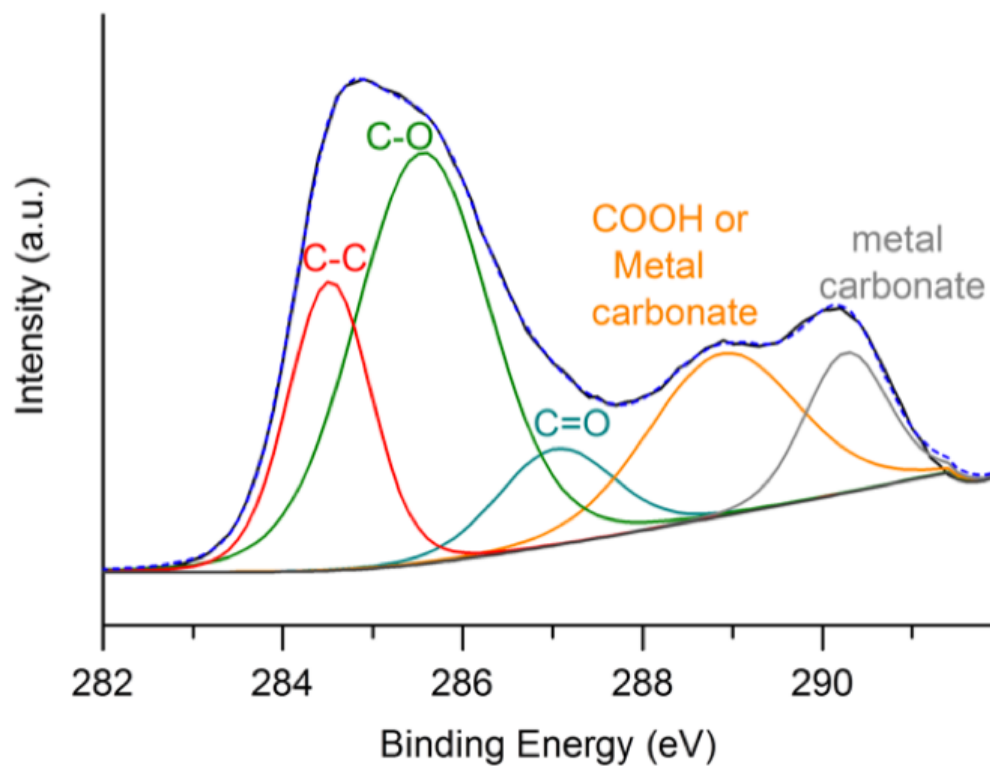


Figure S12. XPS C1s spectra of NHTC after four loops measurement.

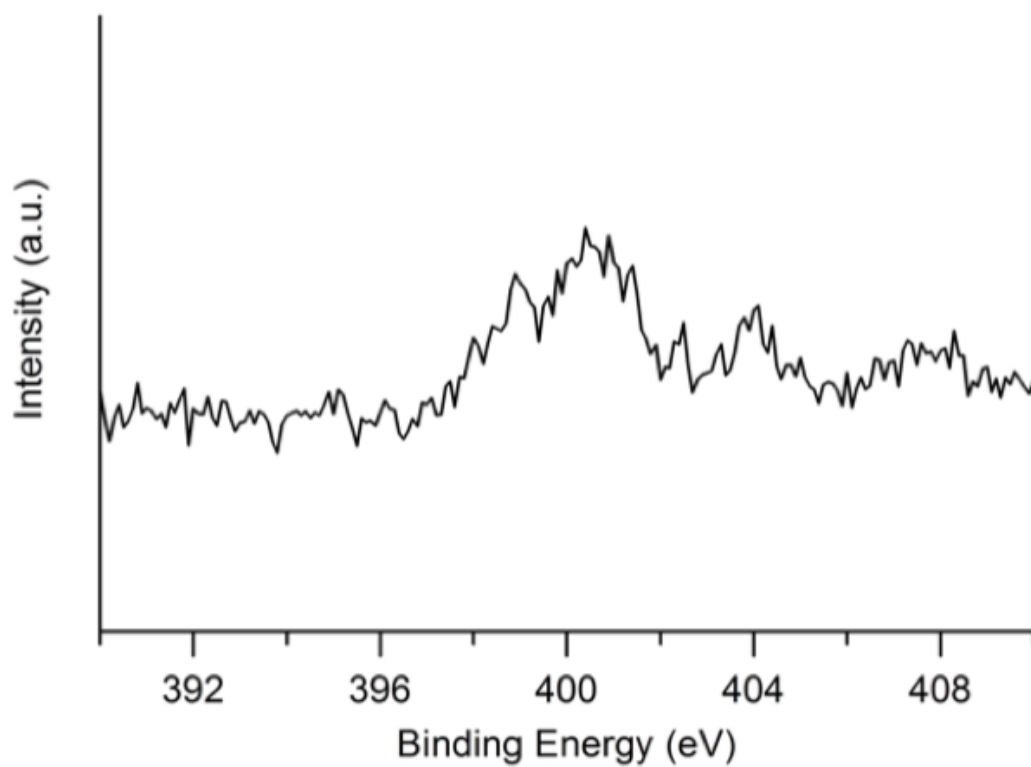


Figure S13. XPS N1s spectra of NHTC after four loops measurement.

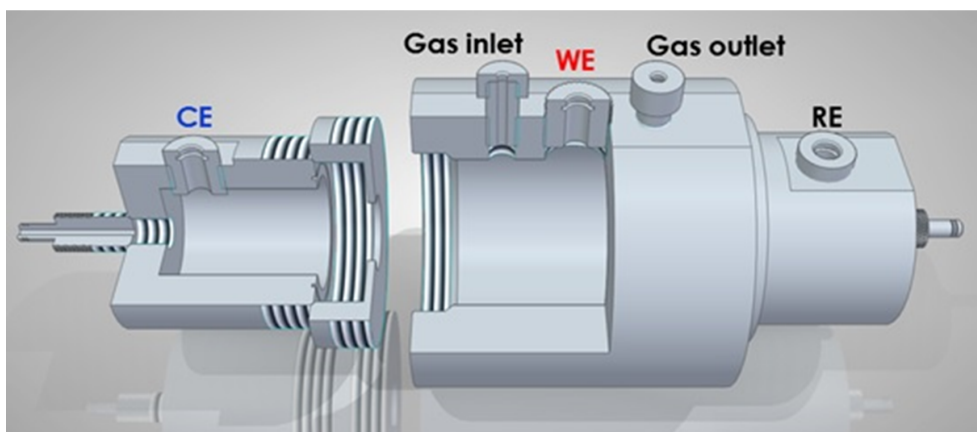


Figure S14. Gas collection cell schematic. CE denotes position for counter electrode, RE reference electrode and in WE the pellet as working electrode is introduced.

For the gas collection experiments, 130 mL of 0.1 M KOH was used as electrolyte, leaving roughly 50 mL volume as the gas phase directly above the liquid. The cell has one gas inlet for Ar purging and one gas outlet for collecting product gas. The counter electrode used in this case is a graphite rod. The cell has the possibility to induce an electrolyte flow as well as to separate the CE and WE compartment, but these options were not used in the present work.

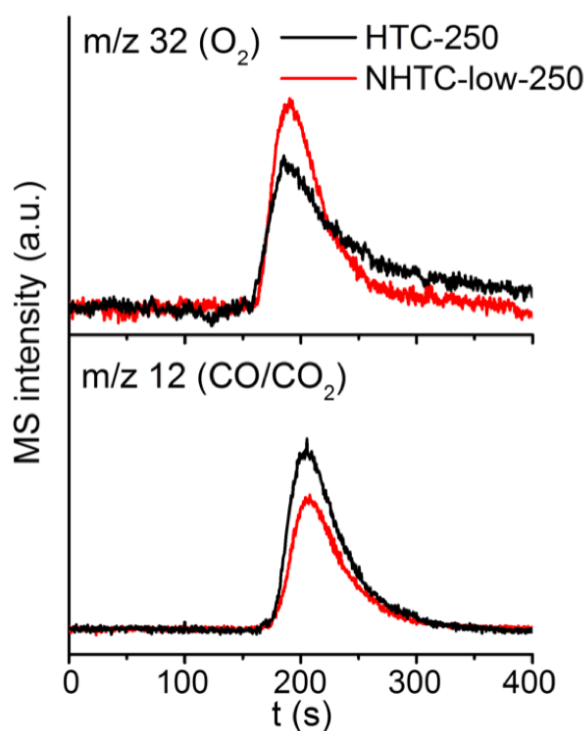


Figure S15. Mass spectrometry profile of $[O_2]^+$ ($m/z = 32$) and $[C]^+$ ($m/z = 32$) corresponding to ion fragmentation of CO/CO₂ for HTC-250 as well as NHTC-low-250 after 18 h of gas product accumulation with an applied potential of 1.8 V.

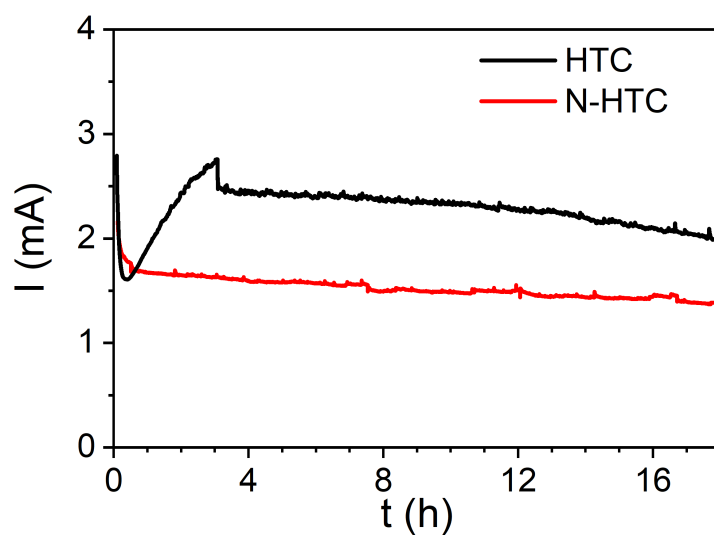


Figure S16. Chronoamperometric measurement at 1.8 V vs. RHE performed in the gas collection cell of HTC and NHTC.

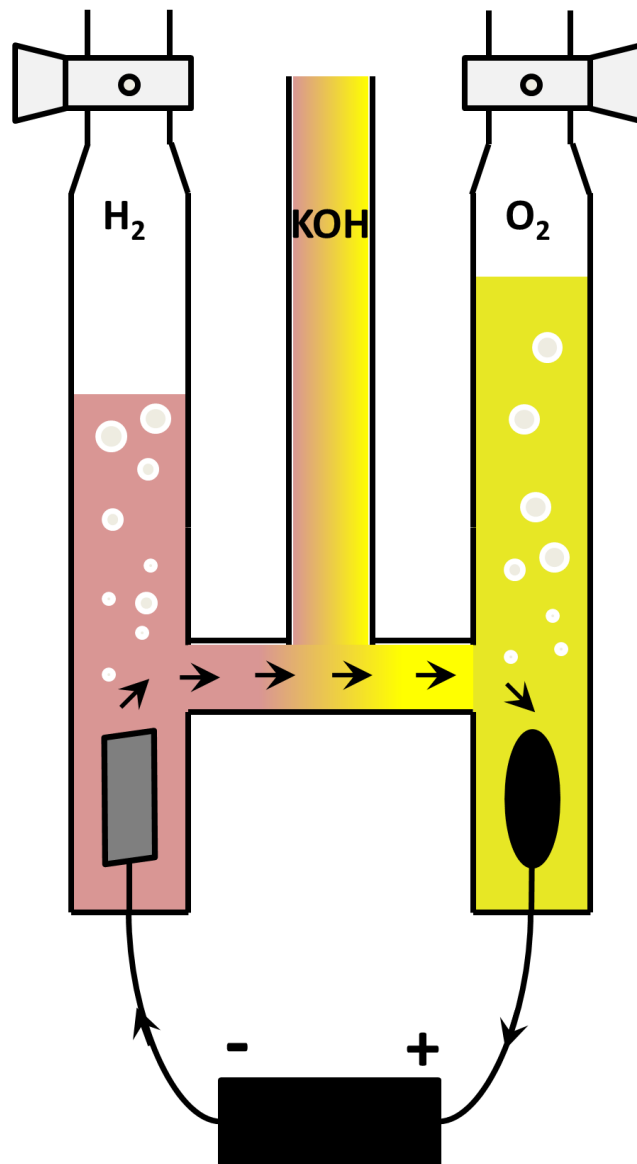


Figure S17. Hofmann apparatus schematic. The cylinders on both sides have engraved scales to facilitate the recording of gas volume.

References

- [1] P. H. Matter, L. Zhang, U. S. Ozkan, *J. Catal.* **2006**, *239*, 83.